Migration of Eurasian Wigeon at Põõsaspea

Antero Lindholm

2026-03-15

Caluta **19**, 2026

Introduction

Cape Põõsaspea in Läänemaa, north-western Estonia, is a well-known site for observing migrating waterbirds, particularly in autumn. During the present century, five full-autumn counts—hereafter referred to as project years—have been conducted in 2004, 2009, 2014, 2019 and 2024 (Ellermaa et al., 2010; Ellermaa et al., 2025; Ellermaa & Lindén, 2015, 2020; Ellermaa & Pettay, 2006). These projects aimed to cover all, or nearly all, daylight hours and to document migration rigorously using half-hour observation periods, recording flock sizes and, when possible, plumage types. These counts have greatly improved our understanding of migration at the site. However, limited resources have resulted in intervals of five years between project seasons, meaning that some information—particularly concerning population trends and short-term fluctuations—has inevitably been lost.

Migration observations have also been conducted during the intervening years, especially in 2020–2023 and 2025 (hereafter intervening years). These observations were less systematic, and the resulting data have, or may have, several limitations:

a) Some days within the core migration period lacked observation activity entirely. However, only 16 such days occurred between 16 August and 31 October during the years considered, and overall seasonal coverage can still be regarded as good.
b) Observation days were often shorter, with many afternoons and evenings missing from the dataset. This is probably the most important difference between the project years and the intervening years.
c) The number of observers was sometimes insufficient to document strong migration events as accurately as during project years, or the number of observers was not recorded.
d) Observation times were usually recorded, but counts were not always separated by hour and were sometimes reported only as daily totals. As

shown later, this limitation is relatively minor in the Põõsaspea dataset.

In this article, the migration of the Eurasian Wigeon *Mareca penelope* is examined. The Wigeon is a dabbling duck and one of the most abundant migrant species passing Põõsaspea. In addition to describing migration patterns, observation efficiency is evaluated with the aim of improving comparability between years using a negative binomial generalized additive model (GAM). The model incorporates both seasonal (day-of-year) and daily (hour-of-day) variation in observed counts, as well as selected weather variables. Model performance is assessed to evaluate how well it represents observed migration dynamics and to discuss the challenges involved in modelling bird migration.

Variation in observed bird numbers among years may arise from several sources:

a) True population fluctuations, which are often the primary focus of study, while other factors introduce noise into the data.
b) Weather conditions, either local (e.g. heat haze or fog affecting detectability) or regional (e.g. wind conditions altering migration routes or potentially increasing nocturnal migration). These factors are difficult to control, particularly those operating at larger spatial scales. Observed totals vary greatly between years (see, for example, Figure 5), and it would be naïve to attribute all variation solely to population changes; detectability clearly plays a substantial role.
c) Observation time, which is controllable and explicitly accounted for in the present study.
d) Observation intensity and quality. During project years, observer numbers and observation quality are assumed to have been sufficient, whereas greater variation likely occurred in other years. Although difficult to quantify directly, some of these effects may be inferred from the modelling results.

Material

Most Eurasian Wigeon migration occurs during the latter half of August and throughout September and October, and only this period is considered in the present study. The seasonal timing of migration for this species is illustrated in Figure 1.

Only birds migrating towards the west or south-west were included in the analysis; local birds and individuals flying towards the east or north-east were excluded. Age and sex information were not used in the analyses, except in Figure 1.

Data from the five project years and the intervening years after 2019 were organised into four variables: day of year, month, hour (defined as the hour during which the observation was made), and the number of birds counted.

Inspection of the intervening-year data indicated that most observations were correctly assigned to hourly intervals, although this cannot be guaranteed in all

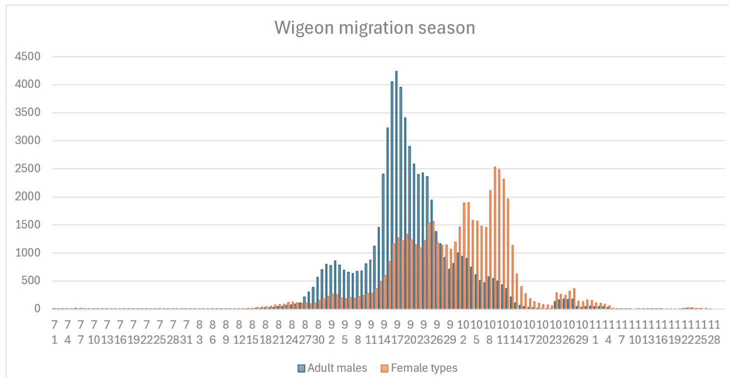

Figure 1: Migration intensity of Eurasian Wigeon during the project years 2004, 2009, 2014, 2019 and 2024. Values represent averages for five-day periods. Adult males and female-type birds (including adult females and first-year individuals) are shown separately. Individuals for which plumage type was not recorded were allocated proportionally according to the distribution of classified birds within each five-day period. The figure shows that the migration season is prolonged and temporally complex due to clear differences in the timing of the various plumage types. It also demonstrates that the period from mid-August to the end of October encompasses the main phase of migration.

cases. This limitation appeared negligible. Only four days contained fewer than five recorded observation rows combined with a ratio of counted birds to rows exceeding 100, and therefore no corrections were applied to the dataset.

As expected, observations were strongly concentrated during daylight hours. To ensure proper circularity in the hourly variable, dark hours with no recorded birds were treated as observed hours with zero counts, which would likely have been the result even if observers had been present. Dark hours were defined as those beginning after sunset or ending before sunrise.

Only fully observed hours were included in the analysis. However, if an observation period was less than ten minutes short of a full hour, the hour was retained. Similarly, if observation continued past sunset or began before sunrise, the hour was considered complete.

In summary, four types of hourly records were distinguished: a) observed hours with a non-zero count, b) observed hours with zero birds, c) unobserved daylight hours, and d) dark hours.

The resulting dataset is uneven and relatively sparse with respect to bird numbers, as many hours contain zero observations. Consequently, the data are highly skewed, characterised by numerous zeros and occasional large migration peaks. Hours of types a), b), and d) were used for model fitting (see next chapter). Figure 2 illustrates the distribution of hour types by year and month.

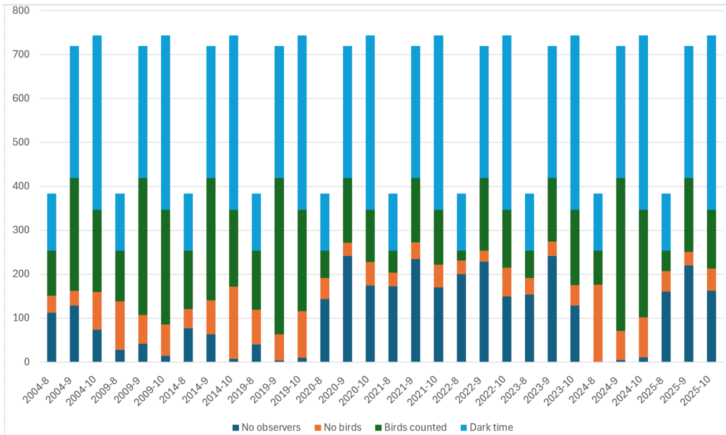

Figure 2: Distribution of dark hours, unobserved hours, and observed hours with and without recorded Eurasian Wigeons by year and month. The contrast between project years and intervening years is clearly visible, and the figure also shows a gradual improvement in observational coverage even among the project years.

Hourly weather data were obtained from the Pakri weather station, located on the northern coast of Estonia approximately 35 km east-northeast of Põõsaspea. A closer station exists at Dirhami, situated just over 2 km southwest of the observation site and clearly visible from it. However, continuous Pakri data are available from 2004 onwards and were therefore used here, following (Lindholm, 2021). At the time of writing, weather data for 2025 were not yet available; consequently, that year was excluded from analyses involving weather variables. The environmental predictors included rainfall, wind direction, and mean wind speed. Weather data were provided by the Estonian Environment Agency (Keskkonnaagentuur, 2026).

The model

The temporal variation in migration counts was modelled using generalized additive models (GAMs) as implemented in the mgcv package in R (R Core Team, 2022; Wood, 2017, 2023). GAMs allow flexible, nonlinear relationships between the response variable and explanatory variables while retaining an additive and interpretable model structure. The response variable was the number of individuals recorded per hour, which consisted of many zeros and occasional very large values. To account for strong overdispersion relative to a Poisson process, we assumed a negative binomial error distribution. A log link function was used so that predictor effects acted multiplicatively on expected migration intensity and model predictions remained strictly positive. Seasonal and diurnal patterns were modelled using smooth functions. Seasonal variation

Table 1: Model definition and diagnostics.

Count ~ te(doy, ihour, bs = c("cc", "cc"), k = c(20, 10)) + te(doy, year_num, bs = c("cc", "tp"), k = c(10, 5)) + s(Rain, k = 10) + s(wind_force, k = 10) + s(wind_dir, bs = "cc", k = 12)

	edf	Ref.df	Chi.sq	p-value
te(doy,ihour)	**111.665**	**170**	**4337.93**	**<2e-16 *****
te(doy,year_num)	**33.582**	**34.946**	**1003.93**	**<2e-16 *****
s(Rain)	**1.353**	**1.626**	**39.77**	**<2e-16 *****
s(wind_force)	**3.095**	**3.896**	**88.78**	**<2e-16 *****
s(wind_dir)	**8.072**	**10**	**317.46**	**<2e-16 *****

was represented by day of year (DOY), and daily variation by hour of day. Both variables are cyclic in nature; therefore, cyclic cubic regression splines were used to ensure continuity between the beginning and end of the daily cycle. The daily pattern changes when the season advances, and not only because the daylight time gets shorter, for some other duck species, see (Lindholm, 2025). To allow the daily migration pattern to change smoothly over the season, the joint effect of day of year and hour was modelled using a tensor product smooth, which permits interaction between the seasonal and diurnal dimensions while respecting their cyclic structure. Because there are changes in the migration phenology over the years (see later), joint effect of day of year and year was also modelled using a tensor product smooth. Additional environmental covariates (rain, wind force, and wind direction) were included as smooth terms to account for weather-related variation in migration intensity. Wind direction was treated as a circular variable and modelled using a cyclic smooth. Model smoothness parameters were estimated using restricted maximum likelihood (REML), which provides stable smoothing parameter estimation and guards against overfitting. Model diagnostics were assessed using standard GAM diagnostic tools, including inspection of effective degrees of freedom, residual patterns, and k-index checks to verify that the chosen basis dimensions were sufficient. Cyclic spline bases were used for day of year, hour of day, and wind direction, with boundary knots specified to enforce periodic continuity at the limits of each circular variable. The definition of the model and the diagnostics are presented in Table 1.

Results and discussion

Figure 3 shows the seasonal distribution of migration as estimated by the model when all years are combined, whereas Figure 4 presents the daily distribution based on observed data from the project years.

Figure 5 and Figure 6 display yearly totals plotted against calendar year treated

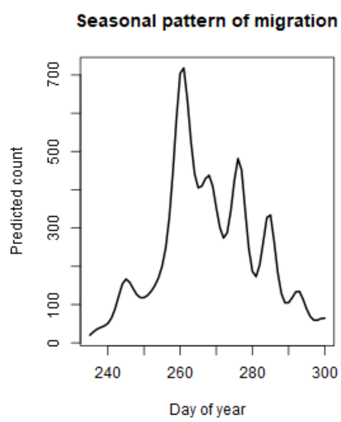

Figure 3: Seasonal pattern from the GAM, years combined.

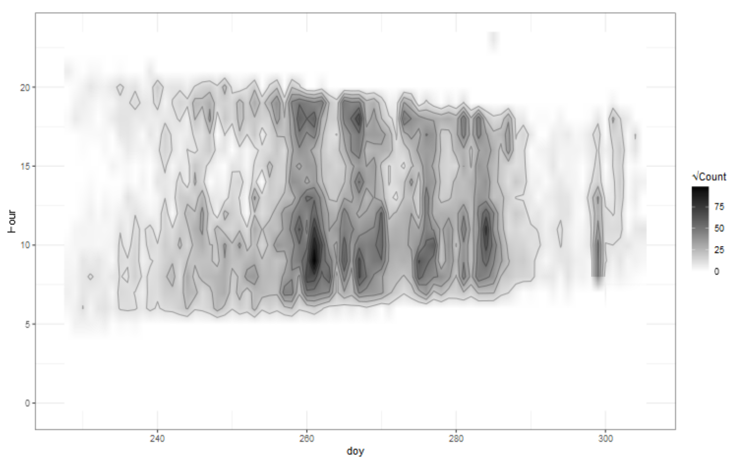

Figure 4: Daily pattern of migration, real numbers from the project years. The daylight time gets shorter, but migration continues with varying strength whole day. The migration is at its weakest around 3pm all the time from August until late October. Daylight saving time shown here, even after it is not in use in late October.

as a continuous variable, thereby preserving the unequal intervals between observation years. Figure 5 presents the observed seasonal totals of Eurasian Wigeon based on the dataset used here, including only fully observed hours as in the model. In Figure 6, observed hours are represented by the actual counts, whereas unobserved hours are replaced by model predictions.

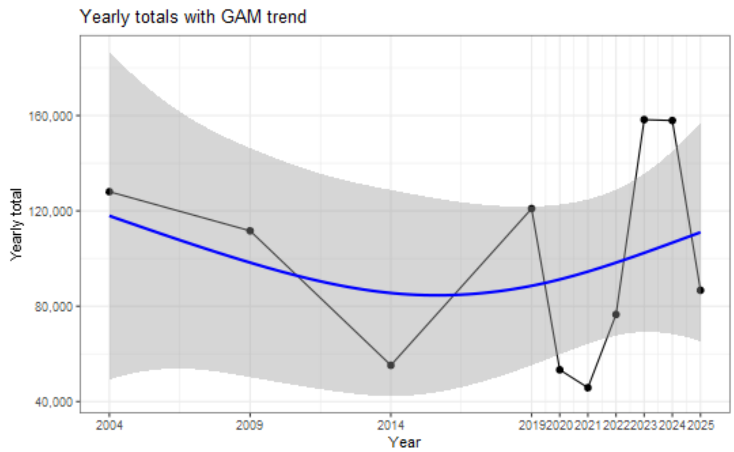

Figure 5: Real counted yearly totals of Eurasian Wigeon.

Meaningful prediction of bird numbers passing a site requires some regularity in the structure of migration. Such structure can be captured and smoothed using a GAM, which can then be applied for prediction. However, as illustrated in Figure 1, migration timing may become more complex when multiple populations use different routes or when sexes and age classes differ in timing, as is common in birds. While the GAM can accommodate complex seasonal distributions and varying migration intensity, it still makes assumptions about the overall seasonal and daily structure across years. Although the model does not assume identical phenology between years, irregular patterns may nevertheless challenge its performance.

Complexities are evident in this real-world case. First, migration timing varies somewhat between years. The mean migration date of Wigeon at Põõsaspea has ranged between 23 September and 1 October during the study period (based on birds observed between 1 July and 5 November). There appears to be a shift towards later migration over time (Figure 7).

Figure 8 - Figure 17 show the daily distribution of counts by year. Although there is a clear main migration period, day-to-day variation within seasons is substantial. A common pattern is the presence of two peaks: one in mid to late September and another well into October. Although these figures show observed numbers, coverage in many years is sufficiently complete that this variability likely reflects real variation in migration intensity—namely, the numbers that could theoretically be observed at the site using standard visual counting methods.

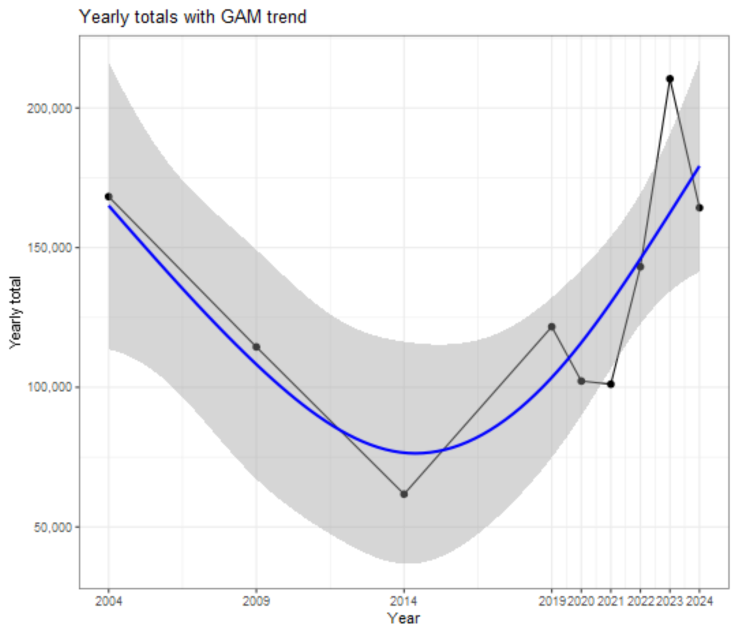

Figure 6: Yearly totals, real counts from the observed hours, predicted counts from GAM for the non-observed hours.

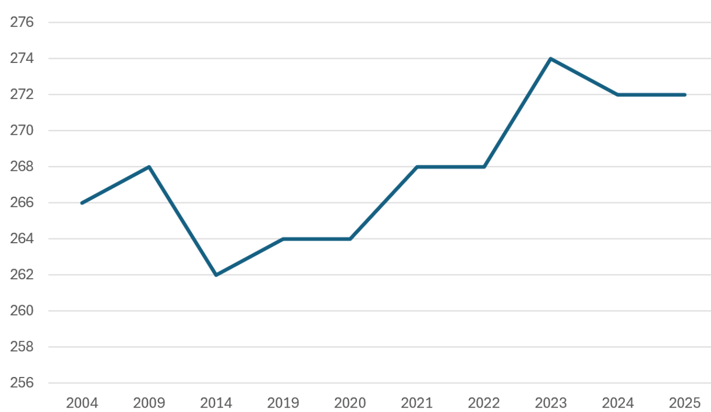

Figure 7: Day of the year of the average Wigeon from year to year.

Thus, if peak migration occurs on different dates in different years, this most likely represents genuine biological variation rather than differences in observation efficiency.

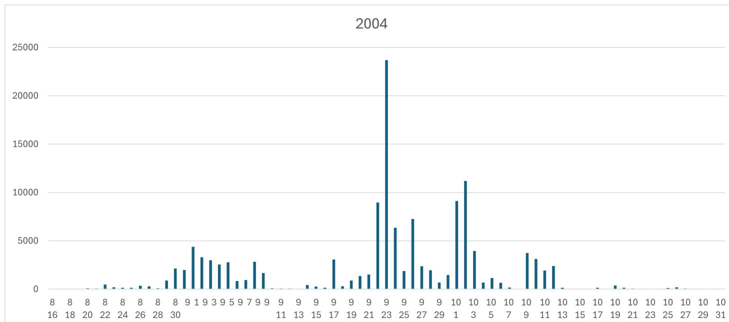

Figure 8: Distribution of the migration in 2004.

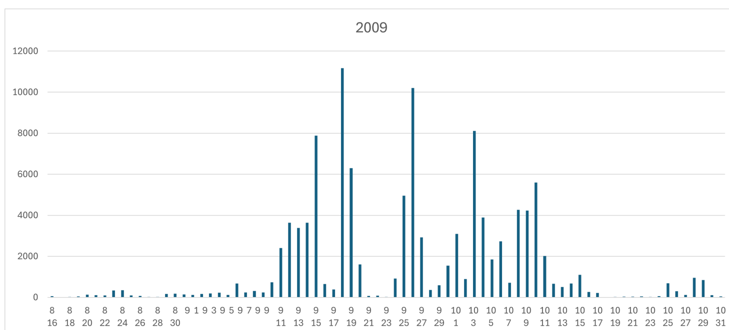

Figure 9: Distribution of the migration in 2009.

As expected, totals from the project years in Figure 6 closely match the observed counts. Model predictions have a larger influence on the intervening years. Overall, trends appear smooth and plausible. However, 2023 stands out as an anomalously strong year. On 2 October 2023, a record 81,409 individuals were counted, accounting for approximately half of the annual total (Figure 15). This exceptional peak complicates model performance: the model predicts approximately 52,000 birds during unobserved hours that year. For example, on 11 October 2023, the unobserved daylight hours between 12:00 and 18:00 are predicted to include over 1,600 birds, although only 57 individuals were counted during the observed forenoon period.

The Gini coefficient measures how unevenly the total number of birds is distributed across the migration season. A value of 0 indicates perfectly even distribution across days, whereas a value close to 1 indicates strong temporal concentration, with most birds passing during a few peak days. Higher Gini values therefore indicate more temporally concentrated migration.

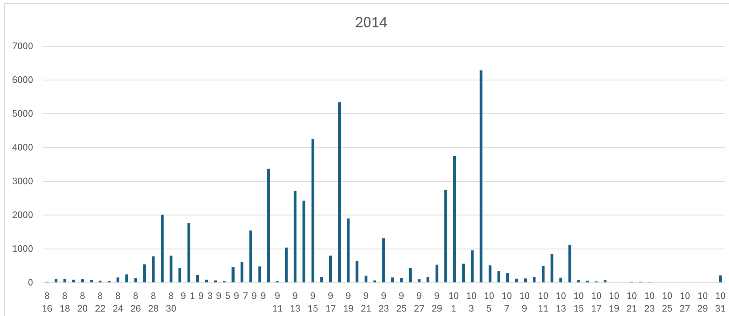

Figure 10: Distribution of the migration in 2014.

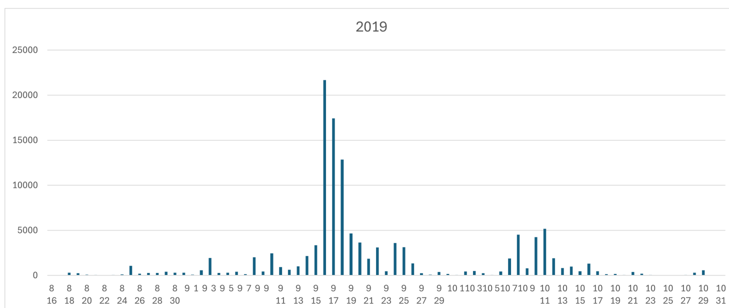

Figure 11: Distribution of the migration in 2019.

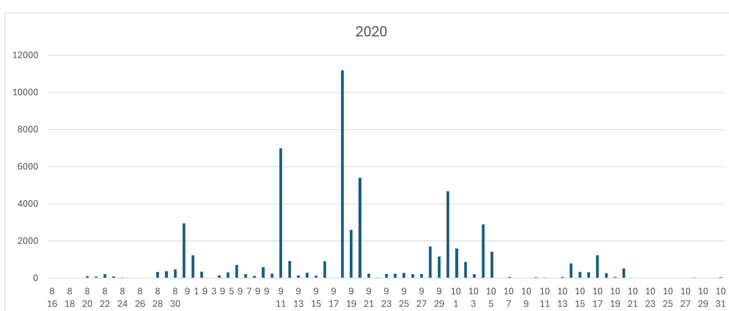

Figure 12: Distribution of the migration in 2020.

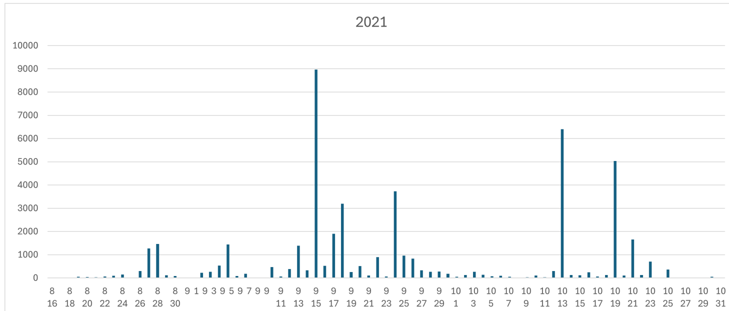

Figure 13: Distribution of the migration in 2021.

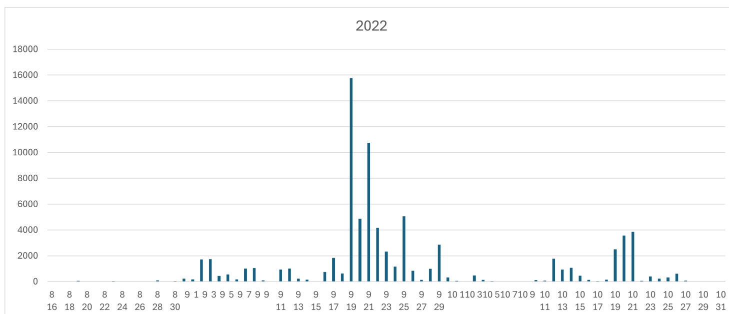

Figure 14: Distribution of the migration in 2022.

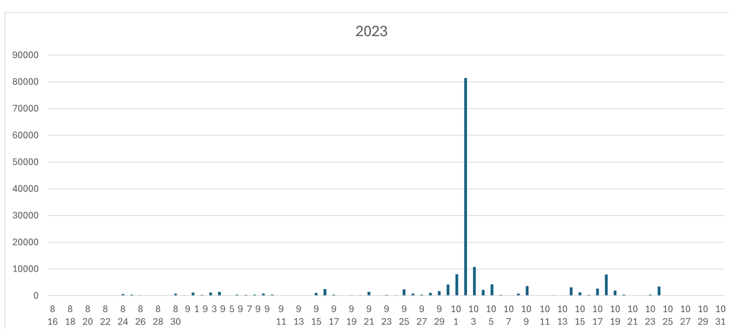

Figure 15: Distribution of the migration in 2023.

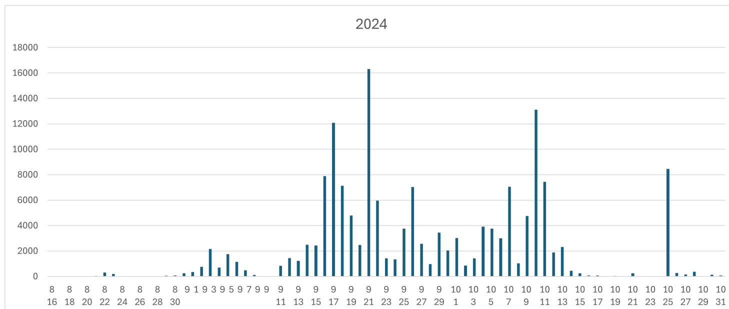

Figure 16: Distribution of the migration in 2024.

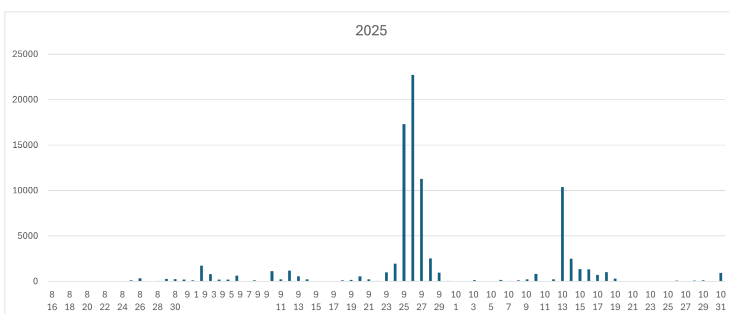

Figure 17: Distribution of the migration in 2025.

Using observed counts only, the Gini coefficient ranges between 0.70 and 0.85 across years (Figure 18). Values are consistently lower in project years than in intervening years, suggesting that reduced observation effort during intervening years caused migration to appear more concentrated into fewer days. Although this effect is not immediately obvious, it likely reflects differences in observation effort. While some days may have had more observers and therefore higher recorded totals, a more plausible explanation is that observation periods were extended during favourable migration days, increasing the apparent concentration of passage.

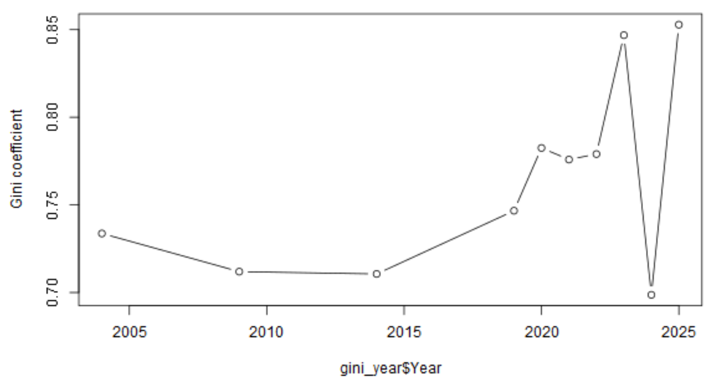

Figure 18: Gini coefficient of the real counted numbers.

When the GAM-adjusted dataset combining observed and predicted counts is used (Figure 19), results differ markedly: migration now appears more concentrated during project years. The Gini coefficient ranges from 0.61 to 0.74, indicating a generally less concentrated distribution after accounting for observation effort. This suggests that the model may slightly overcompensate for differences in effort. As expected, differences between the two approaches are minimal during project years—for example, less than 0.01 in both 2019 and 2024—but substantially larger in intervening years, ranging from 0.13 to 0.17.

Figure 20 shows the length of the 80% migration window based on observed counts, and Figure 21 presents the same metric based on combined observed and predicted counts. Considerable variation is evident, emphasising that the model cannot simply assume a constant migration structure across years. This variability appears to reflect genuine biological differences rather than differences in observer activity.

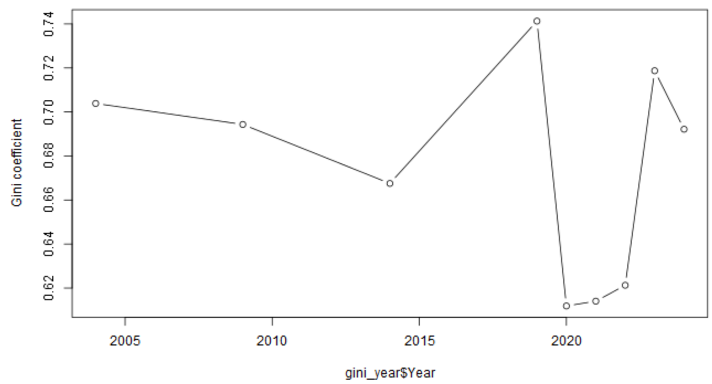

Figure 19: Gini coefficient of the real counted numbers, supplemented with predictions.

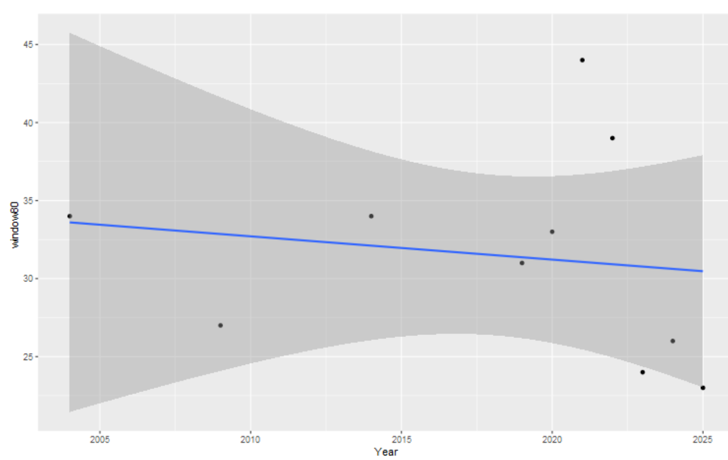

Figure 20: Length of the 80% migration window based on observed counts.

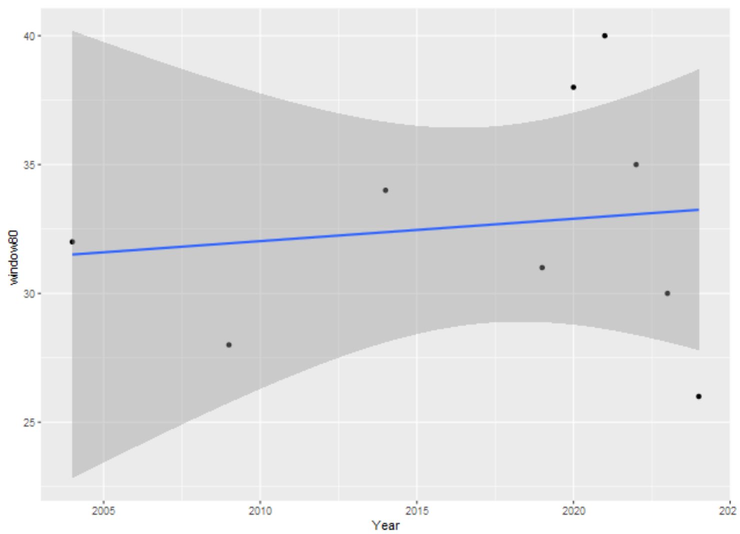

Figure 21: Length of the 80% migration window based on combined observed and predicted counts.

Weather components

See Figure 22 - Figure 24. Weather variables contributed substantially to the model. Wind direction showed the most complex response, indicating strong directional selectivity in migration conditions. Southerly winds were associated with reduced numbers of visibly migrating Wigeon, whereas northerly and north-easterly winds provided the most favourable conditions for observing strong migration. This pattern may not necessarily reflect changes in migration intensity itself, but rather differences in detectability, as strong southerly winds may cause birds to drift farther offshore and thus beyond effective observation range.

Rain showed an approximately linear negative effect on observed migration intensity, although heavy rainfall events were relatively rare. Wind speed also had a negative effect, but this became evident mainly under strong wind conditions, typically exceeding 10 m/s and particularly above 15 m/s.

What is learned about the modelling and data gathering

Because several nearly complete seasons are available, the Põõsaspea dataset is easier to analyse than many other migration datasets. In addition to the project years, the intervening years included in this study were also relatively well documented compared with many other migration sites, particularly during the main Wigeon migration period from mid-August to the end of October. In

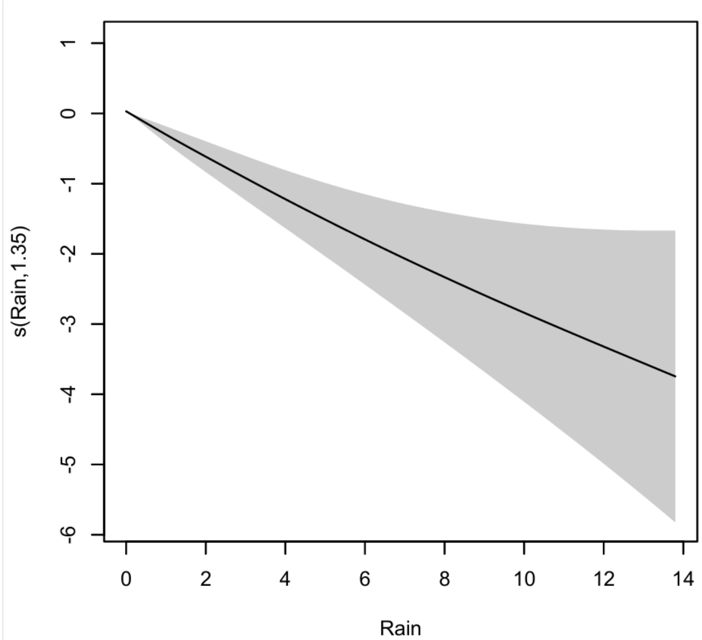

Figure 22: Effect of rain.

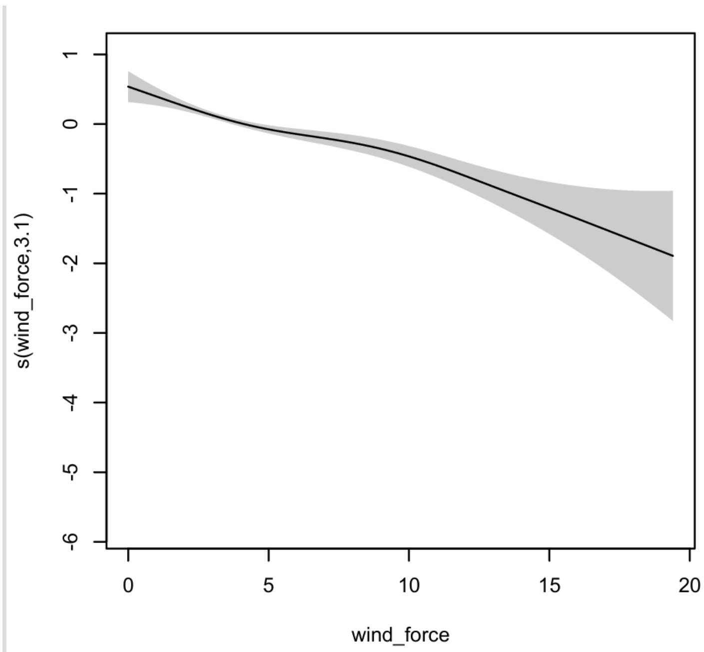

Figure 23: Effect of wind force.

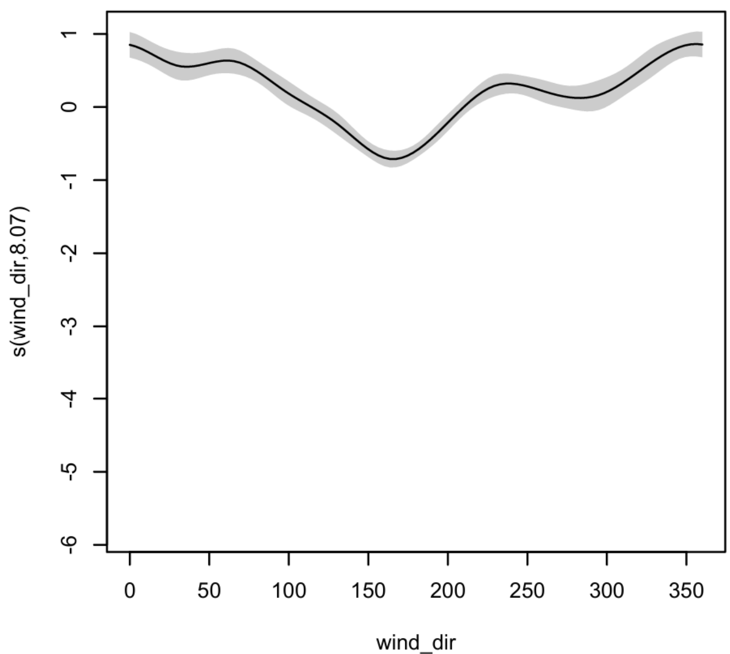

Figure 24: Effect of wind direction.

this study, incomplete years were adjusted using a generalized additive model (GAM) to improve their comparability with the nearly complete seasonal counts. As a result, Figure 6 likely provides a realistic representation of changes in the numbers of Eurasian Wigeon passing the site during autumn migration.

At Põõsaspea, data from some additional years—for example 2015–2018—are so incomplete that prediction was not attempted. At other migration sites, partially observed years may still be usable, even if observation coverage is poorer than in the intervening years analysed here. In such cases, it may be unavoidable to assume similar migration timing between years, although the validity of this assumption should always be evaluated during the analysis.

There are indications that the method applied here may somewhat overcompensate for gaps in observation coverage. The model could therefore be refined in future studies. Furthermore, the approach could be applied to other species with different migration structures. For example, the most abundant species at the site, the Common Scoter *Melanitta nigra*, shows large migration peaks during July evenings, which are less frequently observed in intervening years, meaning that a substantial proportion of the population likely passes undetected.

In any case, applying this type of modelling approach requires that observation times are recorded with sufficient temporal precision. Ideally, most counts—and preferably all—should be divided into hourly intervals (or even finer resolution), as daily activity patterns form an essential component of these analyses. Whenever possible, observations should cover complete time intervals (e.g. full hours when hourly data are used), making it preferable to begin and end observation sessions at exact hour boundaries. Recording the number of observers would also be highly valuable, but this information should be documented separately for each observation interval.

Acknowledgements

Margus Ellermaa has been instrumental in initiating the project and leading it several times. Annika Forsten did most of the migration watching in recent times, especially during the intervening years. Many other counters have contributed.

References

Ellermaa, M., & Lindén, A. (2015). Sügisränne põõsaspeal 2014. aastal. *Hirundo*, *2015*(1), 20–49.

Ellermaa, M., & Lindén, A. (2020). Sügisränne põõsaspeal 2019. aastal. *Hirundo*, *33*(1), 1–29.

Ellermaa, M., Lindén, A., & Forsten, A. (2025). Sügisränne põõsaspeal 2024. aastal. *Hirundo*, *38*(1), 1–27.

Ellermaa, M., & Pettay, T. (2006). Põõsaspean niemen arktinen muutto syksyllä 2004. *Linnut Vuosikirja*, *2005*.

Ellermaa, M., Pettay, T., & Könönen, J. (2010). Sügisränne põõsaspeal 2009. aastal. *Hirundo*, *23*, 21–46.

Keskkonnaagentuur. (2026). *Ajaloolised ilmaandmed*. https://www.ilmateenistus.ee/kliima/ajaloolised-ilmaandmed/

Lindholm, A. (2021). Weather versus bird numbers observed on active migration at põõsaspea neem, estonia. *Caluta*, *12*.

Lindholm, A. (2025). Migration schedules of red-breasted merganser, velvet and common scoter at põõsaspea, estonia. *Caluta*, *18*.

R Core Team. (2022). *R: A language and environment for statistical computing*. R Foundation for Statistical Computing.

Wood, S. N. (2017). *Generalized additive models: An introduction with r* (2nd ed.). Chapman; Hall/CRC.

Wood, S. N. (2023). *Mgcv: Mixed GAM computation vehicle with automatic smoothness estimation*. https://CRAN.R-project.org/package=mgcv